Are there bacteria in the ovules of *Cycas revoluta*? An exploratory study.

University of Victoria Honours Thesis 2020/2021

Department of Biology

Madeline Antony V00885528

Supervisor: Dr. Patrick von Aderkas

Abstract

The presence of bacteria in the ovules of *Cycas revoluta* was examined in three individuals and five tissues via DNA extraction and qPCR. The five tissues examined were: integument, apex of megagametophyte, interior of megagametophyte and chalazal end of the megagametophyte. The extraction process used a modified CTAB method. The average extraction concentrations were 5.13 ng/µL for the nucellus, 206.22 5.13 ng/µL for the apex of the megagametophyte, 83.15 ng/µL for interior, and 249.98 ng/ul for the chalazal end. The integument samples had an extraction average concentration of 190.3 ng/ul. qPCR was done using the Ncl-I, *niH,* 16S and Cycas LFY primers. Each tissue type displayed amplification products for LFY, and none of the tissue types displayed significant amplification for NCI or *niH.* The apex and interior sections of the megagametophyte were the only two tissues to display 16S amplification. It was concluded that there were unidentified bacteria in the apex and interior sections of the megagametophyte of *Cycas revoluta* ovules.

Introduction

Approximately 300 million years ago, in the late Paleozoic or early Mesozoic era, cycads diverged from the common ancestor they shared with the other gymnosperms (Mangka *et al.,* 2020). Based on the fossil record, it is believed that cycads reached their peak diversity, both morphologically and geographically in the Jurassic-Cretaceous (Nagalingum *et al.,* 2011). Since that time, their populations have been declining due to competition with flowering plants, the loss of dinosaurs as dispersal agents and, more recently, human interference (Nagalingum *et al.,* 2011). Currently, there are approximately 350 extant species and subspecies that are distributed in the tropics, but especially the subtropics (Donaldson *et al.,* 2003; Zheng *et al.,* 2017). Cycads seem to bridge the evolutionary transition of pteridosperms to seed-bearing characteristics, retaining features, such as motile sperm and the introduction of clearly gymnosperm features, such as naked seeds (Zheng *et al.,* 2017).

Cycads have been present throughout human history. They were used in ancient ceremonies and as a food source, as well as a medicinal plant across the globe (Jones, 1993). According to Tessier (1793), as quoted by Whiting (1963), Japanese soldiers relied so extensively on the cycad for food, that the removal of the plants from the island was a crime punishable by death. However, in many countries, cycads were reserved for times of hardship, such as drought, war or in the aftermath of tropical storms (Jones, 1993). In the nineteenth century, the value of cycads transitioned from local consumption to commercial exploitation (Donaldson *et al.,* 2003). In 1845, mills were set up in Florida for commercial starch extraction. Overexploitation led to the collapse of the market in 1925, exacerbated by habitat loss and urbanization (Donaldson *et al.,* 2003). Another form of overexploitation was trade. In 1994, Osborne and their colleagues estimated that approximately 3000 cycads were traded each month

from two markets in South Africa (Donaldson *et al.*, 2003). The two most important modern markets for cycads are as ornamental plants in urban landscapes and as specimen plants for plant collection: more than 13 million cycad plants were exported between 1983 and 1999 (Donaldson *et al.*, 2003). Collection of wild cycad populations to meet the demand of this market is considered one of the main human-related causes of the decline in cycad numbers (Donaldson *et al.*, 2003).

The most important family of cycads, in terms of both commercial and scientific attention is Cycadaceae, which is monogeneric for *Cycas* and diverged early from the rest of the cycads (Norstog & Nicholls, 1997). Fossils from the Eocene deposits on China and Japan suggest that *Cycas*-like plants originated on the ancient landmass of Laurasia approximately 12 million years ago (Donaldson *et al.*, 2003; Mangka *et al.*, 2020). *Cycas* spp. have since radiated to the Pacific Islands, Indochina, Australia, Madagascar, and East Africa (Jones, 2002). Within these regions, the species occupy various habitats, such as coastal and near-coastal lowlands and hills. The climate favoured by *Cycas* is generally hot and humid (Zheng *et al.*, 2017). Morphologically, their stems are short, unbranched, and surrounded by leaf traces. These features, as well as their pinnate leaves, bear passing resemblance to palm trees (Nicholls & Norstog, 1997). Farther up, the stem is capped by cataphylls, which serve as environmental protection, and a crown of large fern-like leaves (Norstog & Nicholls,1997; Kaur, 2006).

Cycas are primarily dioecious, meaning each individual is strictly male or female for the entirety of its life, with morphological differences between individuals based on sex (Norstog & Nicholls, 1997). The male cone is comprised of numerous microsporophylls, carrying ~1000 microsporangia on their lower surfaces in *Cycas* (Norstog & Nicholls, 1997). For the females, no cone is formed, and ovules are borne on megasporophylls (Norstog & Nicholls, 1997). The

loose arrangement of the megasporophylls around a stalk is very distinct from other genera and is often referred to as a pseudocone (Cousins & Witkowski, 2017).

As male cones mature, microsporophylls separate to expose pollen sacs on their undersides (Nadarajan *et al.,* 2018). Mature pollen grains consist of three types of cells: prothallial, tube and generative cells (Norstog & Nicholls, 1997). *Cycas* can be either anemophilous, wind pollinated, or entomophilous, insect pollinated (Nadarajan *et al.,* 2018). In the female plants megametophyte, the timing of pollen capture aligns approximately with the free-nuclear gametophyte stage of the ovule (Kaur, 2006). The mature ovules are elliptical, or egg shaped, platyspermic and bilobate, with a colorful exterior (Kaur, 2006; Norstog & Nicholls, 1997). The protective ovular structure, called the integument, can be differentiated into three layers: (1) outer, colored, fleshy sarcotesta (2) middle, stony sclerotesta, and (3) an inner fleshy endotesta (Kaur, 2006; Zhang, 2019). The integument surrounds the nucellus and extends past the nucellus forming the micropylar tube (Kaur, 2006). The nucellus will later secrete a pollination drop and form a pollination chamber (Kaur, 2006). Within the nucellus is a large megaspore mother cell that undergoes meiosis to produce a haploid set of reproductive cells (Norstog & Nicholls, 1997). The megagametophyte develops from one of these cells. This stage, as mentioned previously, is reached concurrently with the maturity and release of the pollen grains.

Cycas Reproduction

Cycas revoluta are both wind- and insect-pollinated and have developed adaptations to optimize both vectors (Kono & Tobe, 2007). Once the insect has been brought to the ovule, or the wind has brought the pollen into its vicinity, the most important capture mechanism is the

pollination drop. Pollination drops are found in all extant gymnosperms and serve primarily as a tool for capture and transport of pollen (Norstog & Nicholls, 1997). Early reports of pollination drops in cycads were made by in the late 1890s by Webber (1897) and Ikeno (1898). When the ovule has reached receptivity, the nucellar beak secretes a complex fluid which exudes from the micropylar tube forming a small protrusion of liquid directly exposed to the external environment (Kaur, 2006). The pollination drops assist in the capture and retention of pollen grains by providing a route for the pollen into the ovule. The non-saccate pollen grains land in the drop, become wetted, swell, and then sink (Gelbart & von Aderkas, 2002). The swelling of the pollen grain eventually leads to the bursting of the exine at the distal end, and the initiation of germination (Gelbart & von Aderkas, 2002; Kaur, 2006).

Once deposited in the pollen chamber at the most interior part of the micropylar chamber, the slow process of pollen tube growth begins (Norstog & Nicholls, 1997). In the early vegetative stages, the tube cell is at the tip of grain, with the generative and prothallial cells tucked behind (Nostrog & Nicholls, 1997). Growth of microgametophyte and expansion of the intine layer of the tube produces a haustorium-like growth penetrating the nucellus (Norstog & Nicholls, 1997). The haustorium then begins to penetrate into the nucellar tissues via enzymatic lysis, deriving nutrients and accumulating starch for the development of the male gametophyte, as it moves through the nucellus tissue (Kaur, 2006). The generative cell begins to enlarge, and two granular bodies, blepharoplasts, appear at opposite sides of the nucleus (Norstog & Nicholls, 1997). The generative cell eventually divides, producing two spermatids (Norstog & Nicholls, 1997). These develop into two sperm that lie side-by-side within the protruding end of the pollen tube (Norstog & Nicholls, 1997; Kaur, 2006).

In preparation for sperm reception, the megagametophyte separates from the overlying nucellus, creating the archegonial chamber (Norstog & Nicholls, 1997). On the floor of this chamber, which is the apex of the megagametophyte, two or three archegonia differentiate (Norstog & Nicholls, 1997; Kaur, 2006). Mature archegonia have a superficial, lower neck cell and a larger central cell (Norstog & Nicholls, 1997). Surrounding the central cell is a single layer of small cells with large amounts of cytoplasm, the archegonial jacket (Norstog & Nicholls, 1997). The neck cell divides repeatedly until four neck cells are present (Kaur, 2006). These neck cells expand and project into the archegonial chamber (Kaur, 2006).

At maturity, the pollen tubes hang from the nucellus that forms the roof of the archegonial chamber. The mature archegonia are present on the archegonial chamber floor (Norstog & Nicholls, 1997). Due to the zooidogamous fertilization style of *Cycas revoluta,* all that is missing is a medium in which the sperm can swim to the archegonia (von Aderkas *et al.*, 2018). Fluid that fills the archegonial chamber is produced by cells at the apex of the megagametophyte mixed with a small amount of material released from the archegonia themselves (von Aderkas *et al.,* 2018). When the archegonial chamber has been filled by the liquid produced by the megagametophyte, the pollen tubes are immersed. After a small delay, the pollen tubes burst (von Aderkas *et al.,* 2018). The archegonial neck cells separate to form a channel that is open to the egg. A white-coloured substance is released that mixes with the chamber fluid to form ACF (von Aderkas *et al.*, 2018). This fluid may play a role in sperm chemotaxis, assisting the sperm in orienting towards its archegonial target (Takaso *et al.,* 2013). From spermatozoid release to their entry into the archegonia is on the scale of minutes (Norstog & Nicholls, 1997). Only one of the spermatozoids fertilizes the egg, regardless of the number that penetrate it (Norstog & Nicholls, 1997). When the first spermatozoid enters the egg

cytoplasm, the sperm nucleus slips out of its spiral band and fuses with the egg nucleus (Norstog & Nicholls, 1997). The proembryo then cellularizes and embryogenesis proceeds in a manner typical of gymnosperms (Norstog & Nicholls, 1997).

The entire process, from pollination to fertilization, is highly regulated and adapted to optimize the probability of successful reproduction. The sexual fluids that dictate much of the reproductive process are not merely random secretions of water, but instead are strictly timed, highly functional, and complex solutions. All three solutions, the pollination drops, the megagametophyte fluid and the archegonial chamber fluid, are aqueous solutions of carbohydrates, amino acids, and proteins (von Aderkas *et al.,* 2018). These constituents play roles in defense and modification of the ovular environment (von Aderkas *et al.*, 2018). Our understanding of the function of these fluids within the context of the ovular environment continues to expand.

Bacteria in Plants

Recently proteomics revealed the first recorded finding of potential bacterial proteins within the ovules of several *Cycas revoluta* individuals harvested from the Japanese island of Okinawa. This finding appears to be the combined result of improved proteomic technology, allowing researchers to find proteins at lower quantities than before, and improved research depth, creating a larger database of proteins to analyze from. However, the sensitivity of the proteomic technology may have reached the level that moves beyond functional readings, into negligible amounts of proteins. The differentiation between oversensitivity and the potential discovery of bacteria within the ovules of *Cycas revoluta* is the focus of the present study.

The discovery of bacteria within *Cycas revoluta* ovules would make the species part of the norm, not the exception. In an evolutionary sense, gymnosperms are surrounded by groups

that have recorded bacterial presence in their aerial tissues; both pteridophytes and angiosperms have been shown to have a bacterial presence within their tissues (Banach *et al.,* 2019; Frank *et al.,* 2017; Alvarez-Perez *et al.,* 2012). Even within the gymnosperm group, specifically conifers, there have been phylum level discoveries of bacteria and fungi in aerial tissues (Hormazabal & Piotelli, 2008; Pirttila *et al.,* 2005; Ulrich *et al.,* 2008; Seiber, 2007). Furthermore, some extant gymnosperms, including cycads, possess an internal cyanobacterial colony within specialized coralloid root structures that assist the plant in nitrogen fixation (Lindblad, 2008). The ability to form coralloid roots is encoded by the genes of the cycad, an ability that is believed to have evolved millions of years ago in response to nutrient-poor soils (Lindblad, 2008; Chang *et al.,* 2019). Once the filamentous cyanobacteria is inside the root, it induces modifications to the growth and development of their host, due to a differentiation of elongated cycad cells (Lindblad, 2008). The precise timing and location of entrance of the cyanobacteria into the roots is not fully understood, but the cyanobacteria themselves have been well studied (Lindblad, 2008). Within the roots of cycads, the most common symbiotic cyanobacteria are members of the genus *Nostoc* (Chang *et al.,* 2019). The main function of these organisms in their symbiotic relationship is nitrogen fixation, but they also are an interesting source of natural bioactive compounds that possesses antibacterial and antimycotic activity (Walther *et al.,* 2020). Furthermore, cyanobacteria produce arabinogalactan-proteins (AGPs) that contribute to plant growth and are also known to have a role in cell signaling in plant-microbe interactions (Chang *et al.,* 2019). In the coralloid root structures other heterotrophic bacteria have been reported, but only in limited populations (Chang *et al.,* 1988). This is believed to be the consequence of the host cycad's defense system, preventing the mass proliferation of microorganisms that are not cyanobacteria (Chang *et al.,* 2019). Communication between the host and the bacterium, most likely through

secondary metabolites, may also influence the ability of other bacteria to overpopulate the cycad tissue (Chang *et al.,* 2019). Therefore, the extensive period of time that cycads have had to establish bacterial associations, combined with the presence of bacteria in closely related groups and within their own roots, points to the potential of bacterial presence within other structures of the cycad, such as the ovule.

Bacteria and fungi can associate with plants within the episphere (outside) or endosphere (inside) (Dastogeer *et al.,* 2020). The episphere includes the rhizosphere, which is the region around the roots that is under the influence of the plants, and the phyllosphere, which is the surface of the above ground plant structures, such as the leaves, stems, or seeds. The endosphere, being inside the plant tissue, is not divided into above or below ground structures, but instead tends to vary by tissue type (Dastogeer *et al.,* 2020). The root endosphere of cycads houses nitrogen-fixing cyanobacteria, while the seed or ovule endosphere is the region of interest for the current study. The presence of an endophytic microbiome can occur via two potential mechanisms: horizontal or vertical transfer (Frank *et al.,* 2017). Horizontally transferred microorganisms are acquired, during the course of a plant's lifetime from the environment. In comparison, vertical transmission occurs between generations via seed (Frank *et al.,* 2017). Though both forms of transmission do exist, the transfer of microorganisms from the environment is more common (Frank *et al.,* 2017). When examining internal tissues, such as the embryo or endosperm, it is more likely that the microorganisms were transmitted vertically, while regions, such as the seed coat, tend to be colonized horizontally (Nelson, 2018). It is possible that certain bacteria are transmitted both vertically and horizontally, and that in particular circumstances, a beneficial endophyte can be passed onto its offspring (Frank *et al.,* 2017). Traits, such as drought tolerance and disease resistance that are conferred via associations

with a particular microorganism group can be passed to the offspring from a mother plant (Trivedi *et al.,* 2020). This means that, for an ovule, microorganisms could have arrived from environmental sources, such as the pollen grains, insect pollinators or the atmospheric exposure of the pollination drop and micropylar canal, or from the internal structures of the plant, which in turn had acquired them from their parent seed. This relationship is then mediated by the circumstances of the individual plant, such as drought and disease, and its mother plant (Trivedi *et al.,* 2020). Therefore, genetic, and environmental variation creates consequential variation between individuals, between species, all the way up to variation between kingdoms. However, it has been observed that plants that are more closely related phylogenetically can show a lower variation in associated microbiome composition, which demonstrates a potential influence of phylogeny of microbiome composition (Dastogeer *et al.,* 2020). Therefore, examining the microbiomes of phylogenetically related groups can help explain the presence or absence of bacteria in cycads.

Due to the carbohydrate-rich composition of cycad sexual fluids, they may be the optimal environment for the proliferation of microorganisms, which is further exacerbated by their direct exposure to the environment for significant periods of time and to insects, which are potential bacterial vectors (Nepi, 2017). However, a rampant proliferation of microorganisms is not seen in similar carbohydrate rich liquids, such as angiosperm nectar, and this is due to diversified defense mechanisms (Nepi, 2017; Coulter *et al.,* 2012). Complex interactions occur between the microbiome, defence mechanisms and the multi-layered surveillance systems, creating either symbiotic responses that promote microbial colonization or immune responses that suppress it (Trivedi *et al.,* 2020). This leads to the small, selective endophyte populations previously recorded in fern and angiosperm fluids that are able to withstand the high osmotic pressure, low

oxygen levels and presence of antimicrobial compounds, such as hydrogen peroxide (Banach *et al.,* 2019; Frank *et al.,* 2017; Alvarez-Perez *et al.,* 2012). There could be a similar situation occurring in the ovule tissue and sexual fluids of cycads.

According to Hardoim (2019) 155 bacterial genera have been detected inside seed tissues of various plant species. The proliferation of any bacteria or fungi within the seed tissue depends on their ability to tolerate an environment that may contain many different antimicrobial compounds and complex compositional dynamics (Nepi, 2017). Sugar-rich environments influence the microbiome based on the types of sugar, water activity and the presence of other compounds (Nepi, 2017). Environmental differences can create dynamic shifts in the osmotic state, which can influence the stability of macromolecular systems (Lievens *et al.,* 2015). Pollination drops and nectar do not have the same main sugar component, which could create variation in the potential microbial ecology (Nepi *et al.,* 2009). Additionally, temperature, pH, nutrition, microbial dispersion, and habitat history also influence microorganism ecology (Lievens *et al.,* 2015). Colonies within temporary substances, such as nectar or retracting pollination drops, are communities with high turnover rates and rapid colonization-extinction rates (Lievens *et al.,* 2015). If the arrival of microbes by pollinators or other vectors is rare, or rates of extinction outpace rates of arrival, a habitable medium may have a relatively limited microbiome. Most commonly, the microorganisms that survive within the seeds are commensals, that have unknown or limited functions within the plant (Hardoim *et al.,* 2015). These are not microorganisms with mutualistic or the opposite, antagonistic effects (Hardoim *et al.,* 2015). They may become functional in particular situations, but for the most part they are not overly active or influential (Hardoim *et al.,* 2015). Some of these opportunistic colonizers can be pathogenic, but disease tends to only occur when they are in combination with other factors

(Seiber, 2007). The most commonly recorded endophytic microorganisms are Proteobacteria, Actinobacteria and Firmicutes, with smaller numbers of the species in the Bacteroidetes (Trivedi *et al.,* 2020; Nelson, 2018). On the species level, *Pseudomonas, Bacillus, Paenibacillus, Micrococcus, Staphylococcus*, *Pantoea,* and *Acinetobacter* have all be recorded (Frank *et al.*, 2017). Among fungi, Epichole and their asexual forms Neotyphodium are most commonly found, especially when unsaturated fatty acids are present (Nelson, 2018). The order of arrival of microorganisms does shape internal community dynamics (Nelson, 2018). The first to arrive experience the "priority effect" that can shape the future community (Lievens *et al.*, 2015; Nelson, 2018). Once endophytic microorganisms are present, they elicit plant defense reactions, referred to as induced systemic resistance. The subsequent higher host tolerance against adverse conditions, pathogens or other invading microorganisms (Hardiom *et al.*, 2015). Induced systemic resistance has been recorded in gymnosperms, specifically in *Pinus* (Bonello *et al.*, 2006).

Vertical transmission of microorganisms may be beneficial for the safety and success of the seedlings (Hardoim, 2019). Seed-borne microbes are often pioneer colonizers of juvenile plants. They may represent the foundation of the plant microorganism ecology, before microorganisms are taken up from the surrounding soil (Escobar Rodriguez *et al.*, 2018). Although, endophytes of seeds may not last long enough to dominate the microbiome of mature plants, they can affect germination, early plant fitness, and survival (Escobar Rodriguez *et al.*, 2018). Endophytic microorganisms can affect many precursors. They degrade sugars, transforming them into compounds difficult to assimilate by other microorganisms (Alvarez-Perez *et al.*, 2012). They also produce alcohols (Alvarez-Perez *et al.*, 2012). Lastly, they release many forms of secondary metabolites that cause further disruption (Alvarez-Perez *et al.*, 2012).

Microorganisms isolated from other gymnosperms have been shown to produce secondary metabolites with strong bacterial and fungicidal activity (Hormazabal & Piotelli, 2008).

Certain microorganisms have, in fact, been evolving with gymnosperms for nearly 300 million years (Seiber, 2007). The community of certain microbial lineages that were associated with a host across a wide range of environments have been termed "core microbiota" (Trivedi *et al.,* 2020). For these core microbiota the antimicrobial immune response of the plant is either not activated or their response only kills a select number of colonizers preventing extreme proliferation (Seiber, 2007). Colonization by non-host-specific, non-core endophytes may increase diversity and adaptability, which in turn may confer benefits in extreme conditions (Seiber, 2007). Overall, the endophytes of angiosperms and non-cycad gymnosperms appear to be mostly harmless colonizers that are passed on from generation to generation either horizontally or vertically.

The lack of reports of an endophytic presence of microorganisms in cycads seed is due to a number of historical factors. Cycads have been understudied when compared to other seed plants. The proteomic software and bacterial databases used in analysis could have been more advanced than those used in previous research. There may have also been an external factor that modified or permitted the endophytic community to proliferate to the point of detection. Hundreds of thousands of individual microbial cells can exist in a cubic meter of air, representing hundreds of unique taxa, many of which could potentially become infiltrators of the *Cycas* ovule (Womack *et al.*, 2010). As mentioned previously, certain bacteria may proliferate, dominate or become active in times of stress or extreme circumstances (Hardiom *et al.,* 2015). It may be the case that these particular individuals from Okinawa were experiencing extraneous or novel circumstances and passed on induced systemic resistance to their offspring seeds in the

form of an endophytic community at the time collections were made. Finally, the detected bacterial proteins may not be functionally significant. As previously mentioned, detection technology has improved extensively. These improvements could have reached a level of sensitivity that is detecting an insignificant quantity of microorganisms. The current study aims to address these potential explanations.

The study of microbiomes is currently expanding, and this study aims to broaden the understanding of endophytes and cycads. The majority of wild cycad populations are either threatened, critically endangered or on the verge of extinction (Xiao, 2004). Therefore, expanding our understanding of their inner workings is important from an academic and conservation standpoint. From a phylogenetic perspective, confirming an endophytic microbial ecology within the seeds of *Cycas revoluta* would be the first confirmed cycad seed endophyte, which would fill the space between the non-root endophytes of ferns, angiosperms and other gymnosperms. Due to the fact that cycads appear to be an exception by lacking an endophytic microorganism community above ground, this study will attempt to determine if this reflects nature.

Materials and Methods

Samples were obtained from Okinawa, Japan in the summer of 2019 and transported to Canada. The samples were dissected, and surface-sterilized by Dr. Patrick von Aderkas, before being stored at -80 ℃ until used. The tissues used in this experiment were taken from the integument and several areas of the megagametophyte: the chalazal, the apex of the pollination chamber, interior, and the nucellus. The location that each tissue was taken from in context of the entire ovule is displayed in Figure 1.

The DNA extraction was a modified high salt, hot CTAB method (Inglis *et al.*, 2018). The CTAB lysis buffer was made with 100mM TrisHCl pH 8.0, 3 M NaCl, 3% CTAB, 20 mM EDTA and 1% (w/v) polyvinylpyrrolidone (PVP-40). Prior to extraction, 1% v/v 2-mercaptoethanol was added and the solution warmed to 65°C to aid with pipetting. Samples were cut down to 50 mg and added to 2.0 mL microtubes. Three steel balls were also added, and these tubes were immersed in liquid nitrogen. The tubes were transferred directly from the liquid nitrogen to the bead mill and were run for two cycles at 5500-2x45-060 using a Precellys Control Device. Once the samples were powdered, the warm CTAB lysis buffer was added at a volume of 1 mL and the samples were resuspended by short vortexing. The tubes were incubated at 65°C for one hour in a hot block, with inversions of the tube completed manually every ten minutes. Samples were allowed to rest at room temperature for five minutes. A volume of 700µL chloroform:isoamyl alcohol (24:1 v/v; CIA) was added to the sample tubes. The tubes were vortexed for ten seconds and placed in a centrifuge at 5,000 x g for ten minutes. The upper aqueous phase was transferred to a new tube. Nucleic acids were precipitated from the separated aqueous phase by the addition of 70 µL of 3 M sodium acetate at pH 5.2 and 462 µL volume of cold isopropanol. Tubes were mixed by inversion and kept at -20℃ for one hour. DNA was pelletized by centrifugation at 13,000 x g for ten minutes. The supernatants were decanted off and tubes were drained by inversion over a paper towel. The pellets were washed by the addition of 1 mL 70% ethanol and the tubes were again centrifuged for ten minutes at 13,000 x g. Supernatants were removed via aspiration and the tubes were left to dry for approximately one hour. Pellets were resuspended in 50 µL of TE buffer and incubated at 37℃ for 30 minutes.

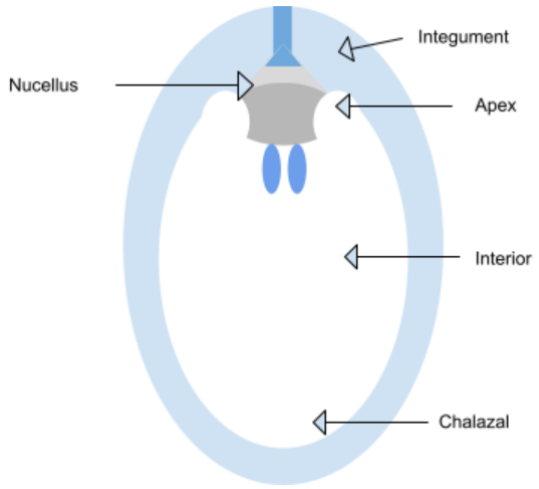

Figure 1 The five tissues used in this study were dissected from three *Cycas* revoluta ovules. The tissues were taken from the nucellus, apex of the megagametophyte, interior megagametophyte, the chalazal end of the megagametophyte, and the integument.

Following extraction and prior to amplification the DNA was stored at -20°C. Quality of extraction was determined using a Thermo Scientific Nanodrop 2000. For the integument samples, a sterilized mortar and pestle was used to grind the tissue, as the bead mill did not yield high concentrations or high quality DNA.

The qPCR method followed instructions provided in the KAPA SYBR Fast qPCR kit. Added to each sample tube was a master mix of 10 mL of SYBR Fast, and 0.4 µL of both the forward and reverse primers. The sample DNA was stored on ice until use. For the experiment, each sample was diluted to approximately 10 ng/µL and 9.2 µL of diluted DNA was added to each tube. The qPCR was run on a Bio-Rad CFX96 Real-Time System and C1000 Thermal Cycler with detection set for SYBR. The qPCR cycle was run at 95 degrees for two minutes for initial denaturation, 95 degrees for three seconds for main denaturation and 60 degrees for 30 seconds for reannealing, then repeated 39 times. A final cycle was run at 95 degrees for five seconds, 65 degrees for five seconds and 95 degrees for 5 seconds for extension. Negative controls for the amplification include a blank tube with only water, a tube with the entire master mix and primers, but no DNA, and a tube with the entire master mix minus the primers and the template DNA. Four primer pairs were run: nifH2, NCl-I, Cycas LFY and 16S (Warshan *et al.,* 2016; Dorn-In *et al.,* 2015; Integrated DNA Technologies, n.d). *nifH*2-F: AACCCGGTGTTGGTTGCGCT, *nifH*2-R: ATGGCCATCATCTCGCCGGA (Warshan *et al.,* 2016), Ncl I-F: CACCGTTCTTCACCTCGCC, Ncl I-R: TGCATACATCGCCATCATTTC (Warshan *et al.,* 2016), Cycas LFY-F: GAGCCTCAGGGAGATAACGC, Cycas LFY-R: ATAAGGCCACTGACTGCACC, and 16S-F: AGA GTT TGA TCC TGG CTC AG, 16S-R: ACG GCT ACC TTG TTA CGA CTT (Integrated DNA Technologies, n.d.). The Cycas LFY

primer pair was hand designed by Dr. Little with the parameters of a GC content of 50-60%, and a base pair number between 75-200.

The melt curve, melt peak, amplification curve and Cq value were collected and analyzed to determine the relative amount of bacteria in the samples compared to the amount of plant DNA. The reference gene for each tissue was Cycas LFY. The limit of detection (LOD) was determined using quarter-dilution samples of *Shewanella* sp., *Pseudomonas* sp., and *Vibrio parahaemolyticus* provided by Drs. Finston and de la Bastide.

Results

DNA Extraction

The average extraction concentrations in ng/µL were 5.13 ± 3.86 for the nucellus, 206.22 ± 87.58 for the apex, 83.15 ± 65.91 for the interior and 249.98 ± 176.45 for the chalazal end of the megametophyte. The integument samples had an extraction average concentration of 190.3 ± 53.54 ng/µL. This method was derived from an optimized protocol for potatoes, and the average extraction concentration found for unsterilized potato samples in our study was 141.55 ng/µL. The extraction values are displayed in Table 1 and 2.

qPCR Amplification

The nucellus had the poorest extraction and also the lowest amplification. There was minimal amplification of the three bacterial primers, NCl-I, *niH*, or 16S. This was determined in comparison to the blank sample, which contained SYBR, nuclease free water and primer, but not template DNA. The non-template blank amplified at similar rates to the template samples (Table 3). In contrast, the *Cycas* primer with template had an average Cq value, or threshold value of

Table 1 Concentrations of DNA (ng/µL) extracted from four tissues of three individual *Cycas revoluta* ovules, as well as the averages. The extractions were completed using a modified CTAB method in a bead mill and the concentrations were determined using a Thermo Scientific Nanodrop 2000.

	Extracted DNA Concentration (ng/µL)			
Tissue Type	Individual 1	Individual 2	Individual 3	Average
Nucellus	1.60	7.85	0.80	5.13 ± 3.86
Apex of the megametophyte	202.70	120.45	295.50	206.22 ± 87.58
Interior of the megametophyte	37.75	52.95	158.75	83.15 ± 65.91
Chalazal of the megametophyte	65.05	268.30	416.60	249.98 ± 176.49

Table 2 Concentrations (ng/µL) of DNA extracted from the integument of an individual *Cycas revoluta* ovules, repeated three times, as well as the average. The extractions were completed using a modified CTAB method in a mortar and pestle, and the concentrations were determined using a Thermo Scientific Nanodrop 2000.

	Extracted DNA Concentration (ng/µL)			
Tissue Type	Sample 1	Sample 2	Sample 3	Average
Integument	185	139.6	246.3	190.3 ± 53.55

Table 3 Absolute amount of DNA in *Cycas revoluta* nucellus tissue and qPCR amplification results. Displayed values include: the total DNA (ng) in the qPCR reaction, the concentration of the DNA in the qPCR reaction (ng/µL) and the Cq values for four primer types: NCl-I, niH, 16S and LFY. The average Cq values for each primer are also displayed, along with the Cq values for the blank samples ran with all components of the qPCR reaction, except for the template DNA. Average values in red represent that the average Cq value for that primer was lower for the template samples than the blank sample. The DNA concentration was diluted to match the requirements for the KAPA SYBR Fast qPCR kit. The qPCR reactions were run on a Bio-Rad CFX96 Real-Time System and C1000 Thermal Cycler with detection set for SYBR.

Nucellus			Primer Type & Cq Values			
Tissue Number	Total DNA (ng)	DNA Concentration (ng/µL)	NCl-I	*niH*	16S	LFY
1	7.36	0.368	33.84	28.36	28.54	30.08
2	9.2000736	0.46000368	34.10	29.72	31.03	32.03
3	10.12	0.506	30.32	27.46	25.42	29.27
Averages			32.75	28.51	28.33	30.46
Blank Cq	0	0	32.37	27.65	25.59	35.13

30.46, which was lower than the blank sample and shows the DNA extracted was of sufficient quality to be amplified. These numbers are supported by the gel (Figure 2). The bands in each of the bacterial primers are light and near the bottom potentially representing the small amount of bacteria that was amplified, background noise or primer dimers. The LFY gene is amplified in two of the samples, but no band is seen for the third which may have been a gel issue, as the qPCR values point to proper amplification.

These results are similar for the amplification and visualization of products extracted from the apex, with the exception of the 16S primer (Table 4). The Cq values for NCl-I and *niH* blanks are lower than the template samples. *niH* is more similar to the blank Cq value, which may indicate some amplification, but very limited. In contrast, the 16S is below or nearly below the Cq value of the respective blank. Based on the reference gene of Cycas LFY, the concentration of 16S amplified products is 0.458 ng/µL. However, since 16S amplifies both plant and bacterial DNA, we cannot distinguish between what is plant and what is bacteria. However, in comparison with other tissues that do not display the same level of 16S amplification, but similar LFY, there is most likely some degree of bacteria present. The gel visualization of the amplified products from the apex tissue showed minimal bands for NCl-I and light bands for the *niH* primer. However, strong, bright bands are seen for the 16S primer, which was expected (Figure 2). The LFY amplification appears similar to the *niH* amplification products and to the other tissues. Again, the LFY primer was used as both a gene for comparison and to ensure the extraction DNA could be amplified.

For the interior tissue, only the LFY primer displayed Cq values for the template lower than the blank (Table 5). The average Cq value for LFY run with template was 31.06, while the blank was 35.16 cycles. Only one tissue did not show any amplification for the NCl-I primer.

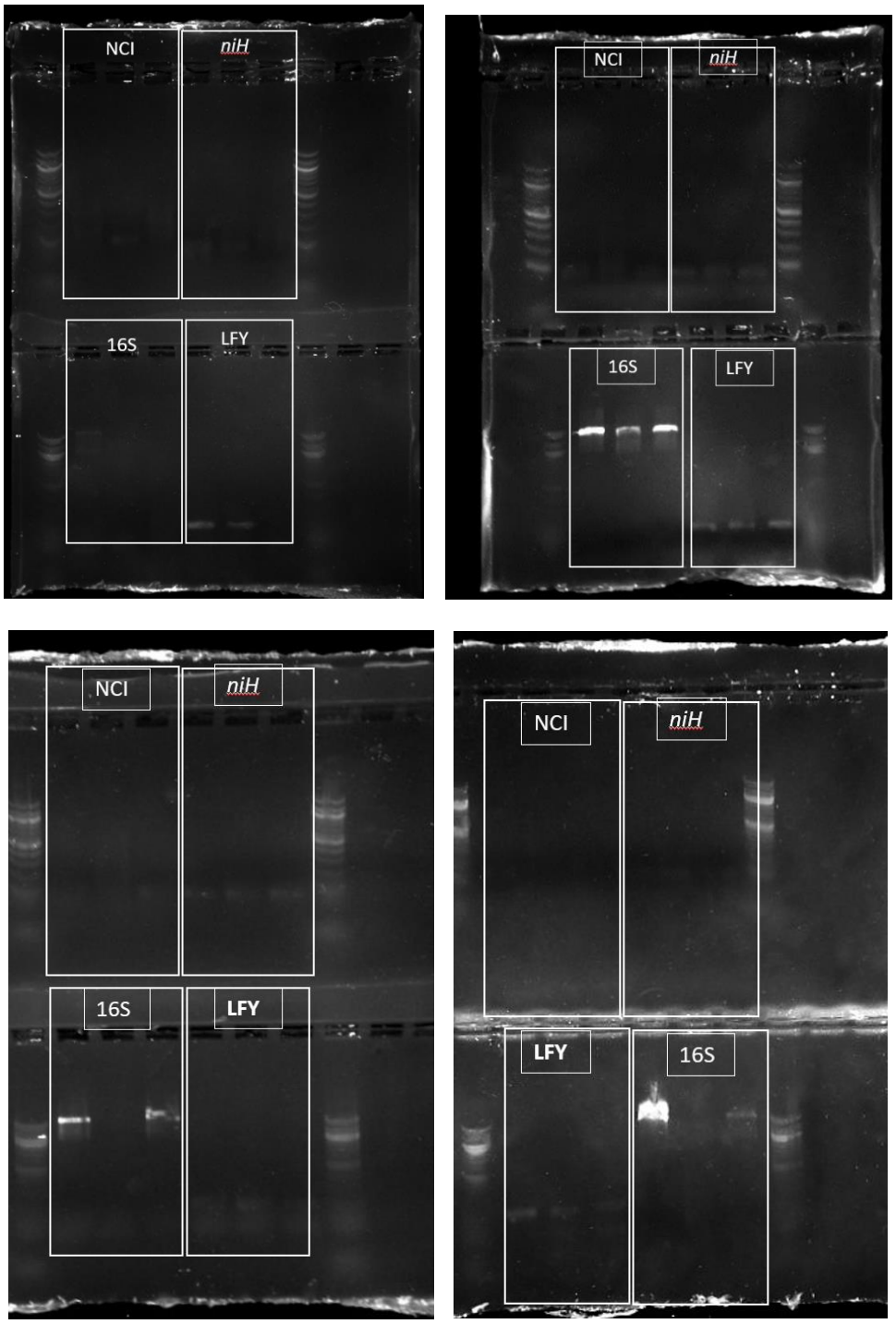

Figure 2 The visualization of the amplified qPCR products for four *Cycas revoluta* ovule tissues gathered from three individuals. Tissue type from top left is nucellus, top right is apex, bottom left is interior and bottom right is chalazal. Each tissue type was run against four primers: NCl-I, *niH*, 16S and LFY. The column with several bands on the outside of the boxes in each gel represents the 50 base pair ladder used as a reference. The bands represent amplified DNA product, with brighter bands representing a greater amplification product. The band position is determined by weight of the product, with heavier products appearing lower in the lane.

Table 4 Absolute amount of DNA in *Cycas revoluta* ovules at the apex end of the megagametophyte tissue and qPCR amplification results. Displayed values include: the total DNA (ng) in the qPCR reaction, the concentration of the DNA in the qPCR reaction (ng/µL) and the Cq values for four primer types: NCl-I, niH, 16S and LFY. The average Cq values for each primer are also displayed, along with the Cq values for the blank samples ran with all components of the qPCR reaction, except for the template DNA. Average values in red represent that the average Cq value for that primer was lower for the template samples than the blank sample. The DNA concentration was diluted to match the requirements for the KAPA SYBR Fast qPCR kit. The qPCR reactions were run on a Bio-Rad CFX96 Real-Time System and C1000 Thermal Cycler with detection set for SYBR.

Apex of the megagametophyte			Primer Type & Cq Values			
Tissue Number	Total DNA (ng)	Dilution Concentration (ng/µL)	NCl-I	*niH*	16S	LFY
1	9.2123096	0.461	34.59	30.23	21.00	28.68
2	9.2026312	0.460	34.65	27.58	25.62	29.75
3	9.188868	0.460	37.46	28.28	22.03	30.08
Averages			35.57	28.70	22.88	29.50
Blank Cq	0	0	32.37	27.65	25.59	35.13

Table 5 Absolute amount of DNA in *Cycas revoluta* ovules in the interior of the megagametophyte tissue and qPCR amplification results. Displayed values include: the total DNA (ng) in the qPCR reaction, the concentration of the DNA in the qPCR reaction (ng/µL) and the Cq values for four primer types: NCl-I, niH, 16S and LFY. The average Cq values for each primer are also displayed, along with the Cq values for the blank samples ran with all components of the qPCR reaction, except for the template DNA. Average values in red represent that the average Cq value for that primer was lower for the template samples than the blank sample. The DNA concentration was diluted to match the requirements for the KAPA SYBR Fast qPCR kit. The qPCR reactions were run on a Bio-Rad CFX96 Real-Time System and C1000 Thermal Cycler with detection set for SYBR.

Interior of the megagametophyte			Primer Type & Cq Values			
Tissue Number	Total DNA (ng)	Dilution Concentration (ng/µL)	NCl-I	*niH*	16S	LFY
1	9.2019872	0.460	N/A	28.81	27.56	31.32
2	9.1995768	0.460	31.63	29.89	32.61	29.96
3	8.869444	0.44	34.93	29.67	26.37	31.89
Averages			33.28	29.46	28.85	31.06
Blank Cq	0	0	32.37	27.65	25.59	35.13

The qPCR products for the interior tissue were similar to the apex, displaying minimal bands for the NCl-I primer, light bands for the *niH* primer and bright bands for the 16S primer (Figure 2). The bright banding in the 16S region was unexpected, based on the qPCR Cq values, but the two samples which display these bands do have the lowest cycle number before reaching threshold. Based on the reference LFY gene and the average Cq values of the interior tissue amplified with 16S, there is approximately 0.388 ng/µL of amplified 16S product, but it cannot be differentiated as bacterial DNA. There is one blank well in the 16S region of the gel, which could be the result of an error in the gel loading. However, the missing sample also displays a higher Cq value than its counterparts and may reflect low amplification of the 16S region for this sample.

With the exception of the LFY primer, the chalazal tissue did not amplify to a significant degree for any of the bacterial primers (Table 6). This was determined by comparing the blank Cq values to the template Cq values. These numbers and conclusions are supported by the gel visualization (Figure 2). The chalazal tissue displayed very minimal bands in any of the bacterial primer categories, NCl-I, *niH* or 16S, with the expectation of an anomalous band in the 16S region. The tissue did amplify, as seen in the light LFY bands that are uniform across the samples and therefore, there appears to be a lack of the target bacteria in this section of the ovule.

The integument displayed significant amplification with the 16S and LFY primers (Table 7). Each of the samples displayed Cq values for the template that were lower than the blank samples. For comparison, the template samples had a concentration of 0.460 ng/µL for host cycad DNA and a concentration of 0.387 ng/µL for the 16S primer. The NCL-I and *niH* primers did not amplify significant products based on their Cq values. As expected, the integument displayed bright bands for the 16S bacterial primer and the reference LFY gene (Figure 3). Based

Table 6 The DNA extraction and qPCR amplification data for three *Cycas revoluta* ovules and their chalazal end of the megagametophyte tissue. Displayed values include: the total DNA (ng) in the qPCR reaction, the concentration of the DNA in the qPCR reaction (ng/µL) and the Cq values for four primer types: NCl-I, *niH*, 16S and LFY. The average Cq values for each primer are also displayed, along with the Cq values for the blank samples ran with all components of the qPCR reaction, except for the template DNA. Average values in red represent that the average Cq value for that primer was lower for the template samples than the blank sample. The DNA concentration was diluted to match the requirements for the KAPA SYBR Fast qPCR kit. The qPCR reactions were run on a Bio-Rad CFX96 Real-Time System and C1000 Thermal Cycler with detection set for SYBR.

Chalazal of the megametophyte			Primer Type & Cq Values			
Tissue Number	Total DNA (ng)	Dilution Concentration (ng/µL)	NCL-I	*niH*	16S	LFY
1	9.15492	0.4575	35.01	28.69	21.16	28.39
2	9.1985684	0.460	31.58	30.09	28.08	32.92
3	9.198528	0.460	36.44	28.67	30.03	30.46
Average			34.34	29.15	26.42	30.59
Blank Cq	0	0	32.37	27.65	25.59	35.13

Table 7 The DNA extraction and qPCR data for one *Cycas revoluta* ovule and three replicates of the integument tissue. Displayed values include: the total DNA (ng) in the qPCR reaction, the concentration of the DNA in the qPCR reaction (ng/µL) and the Cq values for four primer types: NCl-I, *niH*, 16S and LFY. The average Cq values for each primer are also displayed, along with the Cq values for the blank samples ran with all components of the qPCR reaction, except for the template DNA. Average values in red represent that the average Cq value for that primer was lower for the template samples than the blank sample. The DNA concentration was diluted to match the requirements for the KAPA SYBR Fast qPCR kit. The qPCR reactions were run on a Bio-Rad CFX96 Real-Time System and C1000 Thermal Cycler with detection set for SYBR.

Integument			Primer Type & Cq Values			
Tissue Number	Total DNA (ng)	Dilution Concentration (ng/µL)	NCl-I	*niH*	16S	LFY
1	9.1908	0.460	32.07	30.08	21.37	28.71
2	9.1865312	0.460	35.67	29.96	21.38	29.34
3	9.1997976	0.460	36.36	29.01	21.61	29.19
Average			34.7	29.68	21.45	29.08
Blank Cq	0	0	32.37	27.65	25.59	35.13

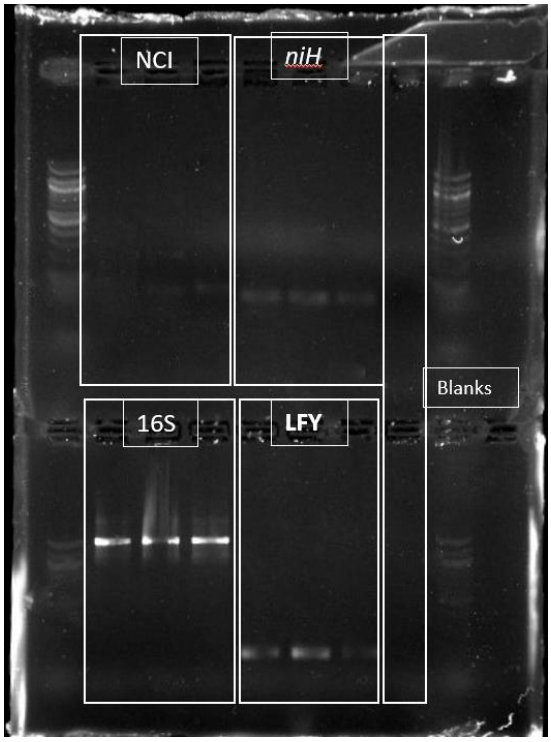

Figure 3 The visualization of the amplified qPCR products for one *Cycas revoluta* ovule integument tissue repeated three times. The tissue was run against four primers: NCl-I, *niH*, 16S and LFY. The white box represents the wells which contained blanks. The column with multiple bands outside of the boxes in each gel represents the 50 base pair ladder used as a reference. The bands represent amplified DNA product, with brighter bands representing a greater amplification product. The band position is determined by weight of the product, with heavier products appearing lower in the lane.

on the banding there appears to be moderate amplification for the NCl-I and *niH* primers, which is not reflected in the Cq values.

In examining the qPCR data, these primers had not been tested on the samples prior to the final experiment. The blanks containing only water or everything, but the primers and template did not show amplification, either through the Cq values or the gel visualization, demonstrating the lack of experiment-wide contamination. The no template blanks did show amplification, but this is expected due to primer dimers and background noise (Figure 4). The melt peak and melt curve for *niH* was irregular, displaying no peak and no curve, respectively (Figure 5). However, the primers were fresh, and the Tm provided was similar to the temperature set for the qPCR reaction. Therefore, the cause of the irregularity is unknown and the results from that primer may be misleading.

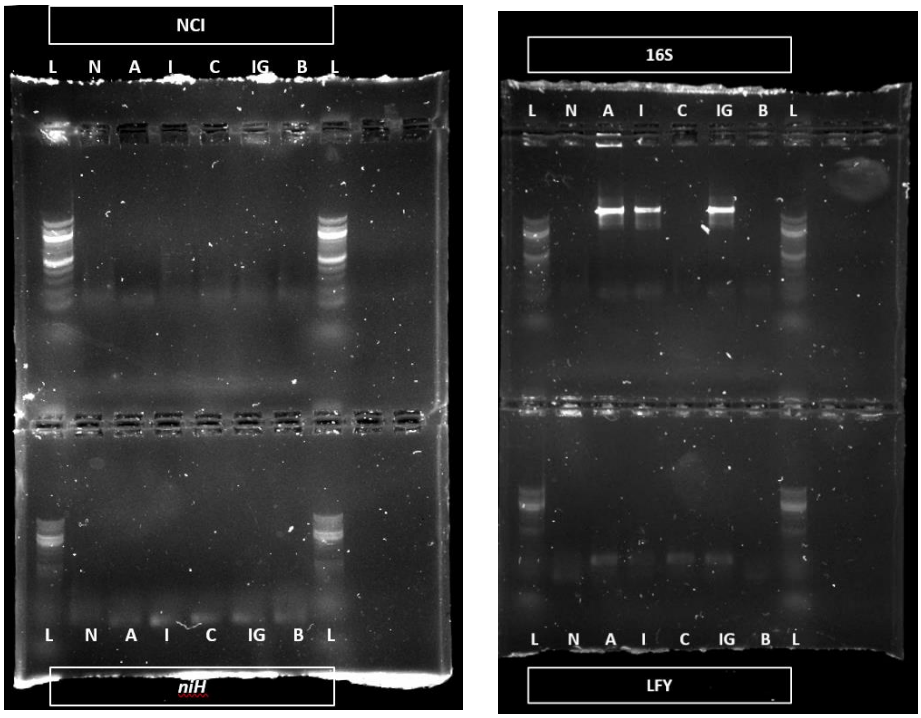

Figure 4 The visualization of the amplified qPCR products for one sample from each tissues type and the no template blank for each primer. The bands represent amplified DNA product, with brighter bands representing a greater amplification product. The band position is determined by weight of the product, with heavier products appearing lower in the lane. The label 'L' represents the 50 base pair ladder in the well below and blanks are represented by the letter 'B'. N= Nucellus, A = Apex of the megagametophyte, I = Interior of the gametophyte, C = Chalazal end of the megagametophyte, IG = Integument.

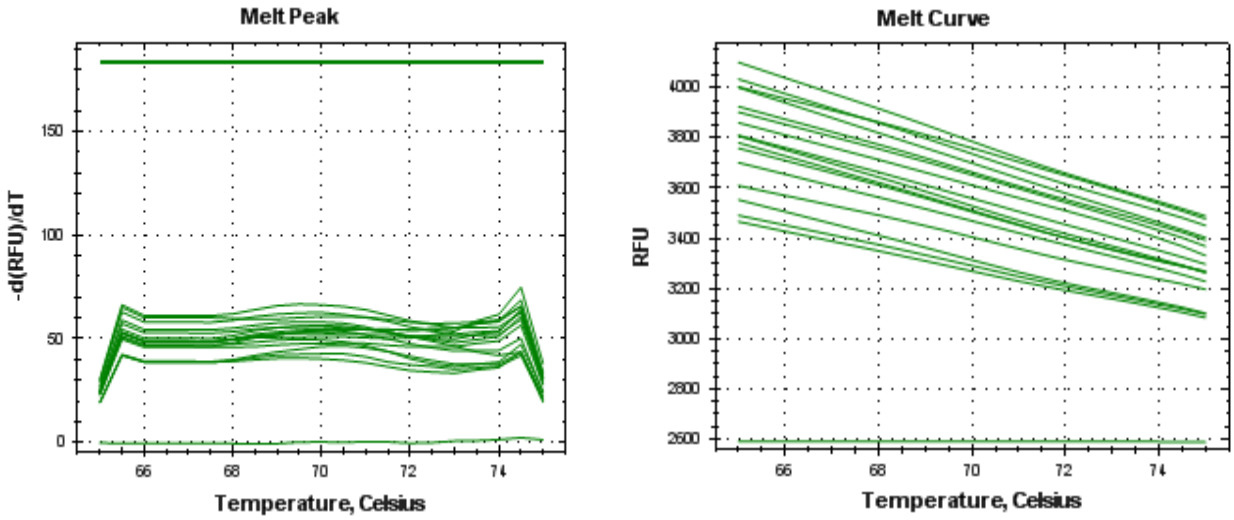

Figure 5 The melt peak (left) and the melt curve (right) for the *niH* primer with each line representing a different sample. Both graphs are irregular, as a peak and curve are expected in each, respectively. The lowest flat line represents the no primer or template blank, which did not amplify, and in the upper lines all 15 template samples are represented. The cause of this abnormality is unknown. RFU = Relative Fluorescence Units.

Discussion

This study has tested a novel DNA extraction method on *Cycas revoluta* ovules and ran the extracted DNA on qPCR to test for the presence of bacteria. Based on these methods, it was concluded that there is most like bacteria in the apex tissue of the megagametophyte, the interior of the megagametophyte, and the integument. None of these bacteria can be identified beyond this classification, but the presence of cyanobacteria in the ovule has been ruled out.

It has been noted in other work on plants endophytes, that technological improvements in genomics and multi-'omics' have enabled the identification and characterization of a greater number of details concerning associated microbiomes (Trivedi *et al.,* 2020; Dastogeer *et al.,* 2020). It is also believed that the traditional method of culturing bacterial communities only reveals a portion of microbial life (Womack *et al.,* 2010; Lievens *et al.,* 2015). An alternative and potentially more accurate method for determining an approximate picture of the microorganisms that are present and their quantity, relative to the surrounding cells, is DNA sequencing (Lievens *et al.,* 2015; Womack *et al.,* 2010). Using sequences of genes, mainly the 16S rRNA gene, revealed a slightly greater diversity in the number of detected bacterial genera than the culture-based approach in work done by Hardoim (2019). DNA degradation tends to be relatively slow in sugar rich environments, which allows a DNA-based detection method to record dead propagules or microbes that were killed in the process of preparation (Lievens *et al.,* 2015). Also, typical surface sterilization techniques kill the organisms on the surface of the tissue, but does remove the DNA (Seiber, 2007). In the current experiment, DNA extraction and qualitative polymerase chain reaction (qPCR) will be the main methods of analysis.

The DNA extraction method used in this study is a modified version of the hot cetyl trimethylammonium bromide (CTAB) method developed by Doyle and Doyle in 1990. The modifications were derived from Inglis and colleagues (2018) to adapt to the high starch and secondary metabolite content of the cycad ovules. The process is a CTAB protocol with a relatively high salt concentration (Inglis *et al.,* 2018). The modification to include 2-mercaptoethanol inhibits polyphenol oxidation, while the polyvinylpyrrolidone binds and removes them (Inglis *et al.,* 2018). Furthermore, cyanobacteria DNA is difficult to extract, due to the production of mucilaginous polysaccharides by the organisms (Walther *et al.,* 2020). The hot CTAB model should account for this carbohydrate interference. The extracted DNA from several tissues within the seed structure was then processed through qPCR. Using qPCR allows for the detection of low-abundance sequences for analysis, observing amplification in real time, and measuring the number of DNA copies you started with (Arduengo, 2019). qPCR combines the sensitivity of conventional PCR and real-time quantification of DNA targets (Chow *et al.,* 2018). The modified high salt, hot CTAB method was used to extract DNA from 4 tissue types and was repeated for three individuals. The four tissue types were nucellus, apex of the megagametophyte, internal tissue of the gametophyte and chalazal material of the gametophyte. Three technical replicates for integument were also acquired using this extraction method. The qPCR primer used were *niH*, which encodes the iron-protein component of the nitrogenase complex in cyanobacteria, NCl-I, which is designed specifically for *Nostoc*, the most prominent cyanobacteria in the root endophytes of cycads, 16S, a universal primer for bacteria, and Cycas LFY, which targeting the LFY gene in *Cycas revoluta* (Warshan *et al.,* 2016; Dorn-In *et al.,* 2015; Integrated DNA Technologies, n.d).

Unlike the other tissues which will be discussed later in this section, the integument tissue was prepared for extraction via grinding by mortar and pestle. This decision was made based on several factors. First, the bead mill did not consistently powder the tissue and would occasionally form a sticky mass that could not be broken down further. This is believed to be the result of resinous compounds being at higher concentrations in certain samples. Secondly, when comparing extracted DNA from integument tissues that did powder in the bead mill and tissues ground in mortar and pestles, the concentration and quality of extractions was higher in mortar and pestle samples. Using an open air grinding method does add an additional stage of potential contamination, but the process was completed in a laminar flow hood and in surface sterilized mortars and pestles. The integument sample extractions were also unique in that they were completed as three technical replicates from one seed versus biological replicates from three individuals, as the other tissues were done. This was done in the context of limited resources and to help mediate the risk of contamination. If there was a significant outlier in the extraction concentration or quality, it would have been due to intra-individual differences, which were not expected to be extremely variable, or contamination. It would not have been due to the variability expected between individuals, seen in biological replicates. The extraction process yielded an average extraction concentration of 190.3 ± 53.54 ng/µL for the three technical replicates. These tissues were then run through qPCR being amplified with each of the primers, NCl-I, *niH,* 16S and Cycas LFY. It was shown that there was significant amplification for 16S and Cycas LFY, but not NCl-I or *niH*. Unfortunately, 16S also amplifies plant tissue DNA, and therefore, we are unable to differentiate the proportion of bacteria amplified. However, the lack of apparent significant 16S amplification in the chalazal does provide support for this amplification to be due in part to bacteria. Using the external integument layer in this experiment

was exploratory and slightly separate from the rest of the tissues. Finding the presence of bacteria for an external layer of a plant would be linked to the phyllosphere, the above ground surface of plant structures on which bacteria can reside. The phyllosphere is a difficult environment for bacteria to colonize, due to the lack of nutrients and protection being provided by the plant. However, it is constantly exposed to the atmosphere which can contain hundreds of thousands of individual microbial cells in a single cubic meter of air (Womack *et al.,* 2010). In locations with high amounts of precipitation, like seen on Okinawa, these colonies are frequently turned-over and replaced. Therefore, our findings are a snapshot of circumstance and may not reflect other times or places.

Within the protective layer of the integument, lies the megagametophyte and its associated tissues. The nucellus tissue, which secretes this pollination drop, was taken through the process of DNA extraction. However, the method was chosen for the carbohydrate-rich tissue of the megagametophyte, not the papery texture of the nucellus. Therefore, between the limited amount of tissue and a non-optimized extraction protocol the yield of the DNA extraction was low. The average extraction concentration was 5.13 ± 3.86 ng/µL, but this concentration is still sufficient for qPCR. The qPCR results showed limited amplification for all three bacterial primers, NCl-I, *niH,* and 16S. There was amplification for the LFY primer, which does verify that the DNA did extract properly and did not interfere with the qPCR process.

The archegonial chamber which sits below the nucellus, is an active part of the ovule. The fluid-forming apex tissue was dissected out of the ovule by Dr. von Aderkas and put through the DNA extraction process in current study. The average extraction concentration was 206.22 ± 87.58 ng/µL. When tested against the four primer types, only 16S and LFY displayed significant amplification, as opposed to NCl-I and *niH*. The concentration of the 16S amplified product was

calculated to be approximately 0.458 ng/µL in relation to the LFY gene and the known concentration of DNA prior to the reaction. Due to the conservation of the 16S gene in plant DNA, the 16S does not solely amplify bacteria, but also host DNA. Therefore, it is impossible at this stage to differentiate between bacterial and plant amplification products. However, as mentioned previously, the lack of significant 16S amplification seen in other tissues does support the presence of some degree of bacteria in the apex tissue of the megagametophyte.

Deeper in the ovule and further into the megagametophyte are the interior tissues and the chalazal end. These regions lie below the archegonium and provide nutrients for the eventual development of the egg. Both areas were examined via DNA extraction and qPCR amplification with the four target primers. The interior region had an average extraction concentration of 83.15 ± 65.91 ng/µL. When amplified, only the LFY primer displayed significant amplification products via Cq values. The gel did confirm the lack of amplification for the NCl-I and *niH,* as well as the amplification of LFY. However, there were bands representing amplified 16S products in two of the samples, that were unexpected based on the Cq analysis. This could represent minor amplification of bacteria that was not present in the third sample. Based on the reference LFY genes and the average Cq values, there is approximately 0.388 ng/µL of amplified product, but it can not be differentiated as bacterial DNA.

With an average DNA extraction concentration of 249.98 ± 176.45 ng/µL, the chalazal tissue showed very limited amplification both in qPCR Cq values and gel visualization. Similar to the interior tissue, only the LFY primer showed significant amplification following qPCR. However, the gel visualization did display one anomalous, bright band representing 16S amplification, which was unexpected and did not match the Cq analysis. This could have been the result of contamination of the sample or an error in gel loading. However, the general

conclusion is that there was no bacteria present in the chalazal end tissue of the megagametophyte.

This study is limited by the nature of the studying minute amounts of bacteria in a novel tissue. Using a universal plant or bacterial primer created complexities in this study, due to the target of bacteria and plants. The evolutionary link between cyanobacteria and chloroplasts consequently creates an overlap in genetic material. Using a universal plant primer on samples of known bacteria, high levels of amplification were seen verifying this genetic overlap. Therefore, any 16S amplification cannot be strictly linked to bacterial presence or host DNA. Also, the kit used in the qPCR reactions uses an intercalating SYBR Fast dye which binds to double stranded DNA. This method is easier to use, more cost efficient and more general than a probe based method. However, the disadvantage is that they bind to any double stranded DNA, including non-specific reaction products which can lead to overestimation of the target concentration (Pabinger *et al.*, 2014). This was partially accounted for by the number of peaks in the melt curve and using a gel for visualization (Adams, 2020). A single DNA species will result in a single peak, but multiple different primer pairs will result in two or more peaks (Adams, 2020). In the gel, any primer dimer binding or odd products should display as a band separate from the target amplified product, but error can still occur. There is also no guarantee that contamination did not occur in any of the stages, however sterile procedure was followed in each step.

Furthermore, high levels of variability in bacteria when compared between locations, both intercontinentally and between plants in the same geographic location (Dastogeer *et al.*, 2020). Therefore, the results of this study are enlightening but limited to the location they were sampled from. There were also no technical replicates, as biological replicates were emphasized,

due to time restrictions. This opens a door for future research. In completing a novel process, this is only the first exploratory look at the world of bacteria in cycads.

In the context of these limitations, it appears that bacterial DNA was found in the apex, interior and integument tissues. The integument was expected to display some level of bacterial presence due to the exposed nature of the tissue and relative lack of requirement for antimicrobial defense systems. The apex and interior tissues were more surprising, due to their enclosed nature and immune system protection. The original expectation for any bacteria present in such internalized tissues was that they would be cyanobacteria, which do have a symbiotic relationship with cycads in their root systems. However, the lack of NCl-I and *niH* amplification in either tissue disproves this theory. As mentioned previously, the *niH* primer did show irregular melt peak and melt curve data, which could mean that some cyanobacteria was missed, due to skewed amplification and this should be addressed in future research. Furthermore, the point of entry for the bacteria into these tissues is also unclear. There was no 16S amplification seen in the chalazal end of the megagametophyte, nor in the nucellus. These would be the two directions of entrance, but bacteria was not seen for either. The more likely direction is from the top, where the micropyle opens to the environment and the pollination drop is eventually exuded. First, the nucellus is a thin tissue separating the apex from this opening and due to the limited DNA that could be extracted from the nucellus there is a chance bacteria is present there as well. Furthermore, there is a stage in development where the apex and nucellus are linked, which could be a point where bacteria is able to imbed in the upper portion of the megagametophyte tissue before the archegonial chamber is formed and the pollination drop is released in the above the nucellus with its antimicrobial properties. Finally, the chalazal did extract well, with the highest average extraction concentration of any tissue tested but did not display significant 16S

amplification. If the direction of invasion were via the lower end of the ovule, potentially via the vascular tissue, we would expect to see bacteria in this region as well. Therefore, the bacteria present in the ovule is most likely the result of horizontal transfer from the environment via the micropyle into the apex and interior of the megagametophyte, with potential infection of the nucellus as well.

Further research should attempt to narrow down the identity of the bacteria present using primers from other genus or species. It would also be beneficial to examine the potential bacteria present on pollen grains in case they are acting as a bacterial vector for ovule invasion. Examination of the vascular tissue within the integument or stem could also further eliminate the entrance of bacteria vertically via this system. Overall, this problem requires a more in depth look to follow the current exploratory study into the bacteria residing in the ovules of *Cycas revoluta.*

Acknowledgements

This work would not have been possible without the help of Dr. Patrick von Aderkas, Dr. Stefan Little, Sarah Lane, Dr. Jürgen Ehlting, Dr. Terri Finston and Paul de la Bastide. Thank you also to the University of Victoria Centre for Forest Biology and the Honors Program.

References

Adams, G. 2020. A beginner's guide to RT-PCR, qPCR, and RT-qPCR. *Biochemist* **42.** doi: 10.1042/BIO20200034.

Alvarez-Perez, S., C.M. Herrera, and C. de Vega. 2012. Zooming in on floral nectar: A first exploration of nectar-associated bacteria in wild plant communities. *FEMS Microbiology Ecology* **80**: 591-602. doi: 10.1111/j.1574-6941.2012.01329.x.

Arduengo, M. 2019. qPCR: The very basics. [Online]. Available: https://www.promegaconnections.com/qpcr-the-very-basics/. [2021, January 11].

Banach, A., A. Kuzniar, R. Mencfel, and A. Wolinska. 2019. The study of the cultivable microbiome of the aquatic fern *Azolla filiculoides* L. as a new source of beneficial microorganisms. *Applied Sciences* **9**: 1-20. doi: 10.3390/app9102143.

Bonello, P., T.R. Gordon, D.A. Herms., D.L. Wood, and N. Erbilgin. 2006. Nature and ecological implications of pathogen-induced systemic resistance in conifers: A novel hypothesis. *Physiological and Molecular Plant Pathology* **68**: 95-104. doi:10.1016/j.pmpp.2006.12.002.

Coulter, A., B.A.D. Poulis, and P. von Aderkas. 2012. Pollination drops as dynamic apoplastic secretions. *Flora: Morphology, Distribution, Functional Ecology of Plants* **207**: 482-490. doi: 10.1016/j.flora.2012.06.004.

Chang, A.C, T. Chen, N. Li, and J. Duan. 2019. Perspectives on endosymbiosis in coralloid roots: Association of cycads and cyanobacteria. *Frontiers in Microbiology* **10.** doi: 10.3389/fmicb.2019.01888.

Chang, D.C, Grobelaar, N., and Coetzee, J. 1988. SEM observations on cyanobacteria-infected cycad coralloid roots. *South African Journal of Botany* **54**: 491-495. doi: 10.1016/s0254-6299(16)31284-4.

Chow, Y.Y., S. Rhaman, and A. Su Yien Ting. 2018. Interaction dynamics between endophytic biocontrol agents and pathogen in the host plant studied via quantitative real-time polymerase chain reaction (qPCR) approach. *Biological Control* **125**: 44-49. doi: 10.1016/j.biocontrol.2018.06.010.

Cousins, S.R., and Witkowski, E.T.F. 2017. African cycad ecology, ethnobotany, and conservation: A synthesis. *The Botanical Review* **83**: 152-194.

Dastogeer, K.M.G., F.H. Tumpa, A. Sultana, M.A. Akter, and A. Chakraborty, A. 2020. Plant microbiome: An account of the factors that shape community composition and diversity. *Current Plant Biology* **23.** doi: 10.1016/j.cpb.2020.100161.

D'haene, B., J. Vandesompele, and J. Hellemans. 2010. Accurate and objective copy number profiling using real-time quantitative qPCR. *Methods* **50:** 262-270.

Donaldson, J.S., K.D. Hill, and D.W. Stevenson. 2003. Cycads of the world: An overview. Pp. 3-8 in Cycads: Status survey and conservation action plan, J. Donaldson, eds., IUCN, Gland and Cambridge.

Dorn-In, S., R. Bassitta, K. Schwaiger, J. Bauer, and C.S. Holzel. 2015. Specific amplification of bacterial DNA by optimized so-called universal bacterial primers in samples rich of plant DNA. *Journal of Microbiological Methods* **113**: 50-56. doi: 10.1016éj.mimet2015.04.001

Doyle, J.J., and J.L. Doyle. 1990. Isolation of plant DNA from fresh tissue. *Focus* **12**: 13-15.

Escobar Rodriguez, C., B. Mitter, M. Barret, A. Sessitsch, and S. Company. 2018. Commentary: Seed bacterial inhabitants and their routes of colonization. *Plant and Soil* **422**: 129-134.

Frank, A.C., J.P. Saldierna Guzman, and J.E. Shaw. 2017. Transmission of bacterial endophytes. *Microorganisms* **5**: 3-21**.** doi: 10.3390/microorganisms50400/70.

Gelbart, G., and P. von Aderkas. 2002. Ovular secretions as part of pollination mechanisms in conifers. *Annals of Forest Science* **59**: 345-357. doi: 10.1051/forest:2002011.

Hardoim, P. 2019. The ecology of seed microbiota. Pp. 103-127 in Seed Endophytes, S.K. Verma, and J.F. White, eds., Springer, Switzerland.

Hardoim, P.R., L.S. van Overbeek, G. Berg, A.M. Pirttila, S. Compant, A. Campisano, M. Doring, and A. Sessitsch. 2015. The hidden world within plants: Ecological and evolutionary considerations for defining functioning of microbial endophytes. *Microbiology and Molecular Biology Reviews* **79**: 293-320. doi: 10.1128/MMBR.00050-14.

Hormazabal, E., and E. Piotelli. 2008. Endophytic fungi from Chilean native gymnosperms: Antimicrobial activity against human and phytopathogenic fungi. *World Journal of Microbiology and Biotechnology* **25**: 813-819.

Ikeno, S. 1898. Untersuchungen ueber die entwickelung der geschlechtsorgane und den vorgang der befruchtung bei *Cycas revoluta. The Journal of the College of Science* **12**: 151-214.

Inglis, P.W., M.R. Pappas, L.V. Resende, and D. Grattapaglia. 2018. Fast and inexpensive protocols for consistent extraction of high quality DNA and RNA from challenging plant and fungal samples for high-throughput SNP genotyping and sequencing applications. *Plos ONE* **13**: e0206085.

Integrated DNA Technologies (n.d.) ReadyMade Primers. [Online]. Available: https://www.idtdna.com/pages/products/custom-dna-rna/readymade-inventoried-oligos/readymade-primers. [2021, March 31].

Jones, D. 1993. Cycads of the World. Reed Books, Australia.

Jones, D. 2002. Cycads of the World, 2nd ed. Smithsonian, Washington.

Kaur, D. 2006. Diversity of seed plants and their systematics: Gymnosperms II (Morphology, anatomy and life cycle of *Cycas, Pinus, Ephedra*). Pp 1-35, Maitreyi College, University of Delhi.

Kono, M., and H. Tobe. 2007. Is *Cycas revoluta* (Cycadaceae) wind- or insect-pollinated? *American Journal of Botany* **94**: 847-855.

Lievens, B., J.E. Hallsworth, M.I. Pozo, Z.B. Belgacem, A. Stevenson, K.A. Willems, and H. Jacquemyn. 2015. Microbiology of sugar-rich environments: Diversity, ecology and system constraints. *Environmental Microbiology* **17**: 278-298. doi: 10.1111/1462-2920.12570.

Lindblad, P. 2008. Cyanobacteria in symbiosis with cycads. Pp. 225-233 in Prokaryotic Symbionts in Plants, K. Pawlowski, eds., Springer, Berlin.

Mangka, L.T., K. Yessoufou, T. Mugwena, and M. Chitakira. 2020. The cycad genus *Cycas* may have diversified from Indochina and occupied its current ranges through vicariance and dispersal events. *Frontiers in Ecology and Evolution* **8.** doi: 10.3389/fevo.2020.00044.

Manthey, F.A. 2016. Starch: Sources and processing. Pp. 160-164 in *Encyclopedia of Food and Health,* B. Caballero, P.M. Finglas, and F. Toldra. Elsevier, Amsterdam.

Nadarajan, J., E.E. Benson, P. Xaba, K. Harding, A. Lindstrom, J. Donaldson, C.E. Seal, D. Kamoga, E.M.G. Agoo, N. Li, E. King, and H.W. Pritchard. 2018. Comparative biology of cycad pollen, seed and tissue: A plant conservation perspective. *The Botanical Review* **84**: 295-314.

Nagalingum, N.S., C.R. Marshall, T.B. Quental, H.S. Rai, D.P. Little, and S. Mathews. 2011. Recent synchronous radiation of a living fossil. *Science* **334**: 796-799. doi: 10.1126/science.1209926.

Nelson, E.B. 2018. The seed microbiome: Origins, interactions and impacts. *Plant and Soil* **422:** 7-34. doi: 10.1007/s11104-017-3289-7.

Nepi, M. 2017. New perspectives in nectar evolution and ecology: Simple alimentary reward or a complex multi-organism interaction? *Acta Agrobotanica* **70**:1704. doi:10.5586/aa.1704.

Nepi, M., P. von Aderkas, R. Wagner, S. Mugnaini, A. Coulter, and E. Pacini. 2009. Nectar and pollination drops: How different are they? *Annals of Botany* **104**: 205-219. doi: 10.1093/aob/mcp124.

Norstog, K.J., and T.J. Nicholls. 1997. The Biology of Cycads. Cornell University Press, Ithaca.

Pabinger, S., A. Dander, M. Fischer, R. Snajder, M. Sperk, M. Efremova, B. Krabichler, M.R. Speicher, J. Zschocke, and Z. Trajanoski. 2014. A survey of tools for variant analysis of next-generation genome sequencing data. *Briefings in Bioinformatics* **15:** 256-278. doi: 10.1093/bib/bbs086.

Pirtilla, A.M., H. Pospiech, H. Laukkanen, R. Myllyla, and A. Hohtola. 2005. Seasonal variations in location and population structure of endophytes in buds of Scots pine. *Tree physiology* **25**: 289-297. doi: 10.1093/treephys/25.3.289.

Seiber, T.N. 2007. Endophytic fungi in forest trees: Are they mutualists? *Fungal Biology Reviews* **21**: 75-89. doi: 10.1016/j.fbr.2007.05.004.

Takaso, T, Y. Kimoto, J.N. Owens, M. Kono, and T. Mimura. 2013. Secretions from the female gametophyte and their role in spermatozoid induction in *Cycas revoluta. Plant Reproduction* **26**: 17-23. doi: 10.1007/s00497-012-0204-5.

Tessier, H.S., A. Thouin, and L.A.G. Bose. 1793. Encyclopedia Methodique on par odre de Matieres Agriculture **3**: 202.

Trivedi, P., J.E. Leach, S.G. Tringe, T. Sa, and B.K. Singh. 2020. Plant-microbiome interactions: From community assembly to plant health. *Nature Reviews* **18**: 607-621. doi: 10.1038/s41579-020-0412-1.

Ulrich, K., T. Stauber, and D. Ewald. 2008. *Paenibacillus:* A predominant endophytic bacterium closing tissue cultures of woody plants. *Plant Cell, Tissue and Organ Culture* **93**: 347-351. doi: 10.1007/s11240-008-9367-z.

von Aderkas, P., N.A. Prior, and S.A. Little. 2018. The Evolution of Sexual Fluids in Gymnosperms from Pollination Drops to Nectar. *Frontiers in Plant Science.* doi: 10.3389/fpls.2018.01844.

Walther, J., A. Schwarz, M. Witthohn, D. Strieth, K. Muffler, and ulber, R. 2020. A qPCR method for distinguishing biomass from a non-axenic terrestrial cyanobacteria cultures in hetero- or mixtrophic cultivations. *Journal of Applied Phycology* **32:** 3767 - 3774.

Warshan, D., G. Bay, N. Nahar, D.A. Wardle, M.C. Nilsson, and U. Rasmussen. 2016. Seasonal variation in *niH* abundance and expression of cyanobacterial communities associated with boreal feather mosses. *The ISME Journal* **10**: 2198-2208.

Webber, H.J. 1897. Structures occurring in the pollen tube of *Zamia. Botanical Gazette* **23**: 453-459.

Whiting, M.G. Toxicity of cycads. *Economic Botany* **17**: 270-302.

Womack, A.M., B.J.M. Bohannan, and J.L. Green. 2010. Biodiversity and biogeography of the atmosphere. *Philosophical Transactions of the Royal Society B: Biological Sciences* **365**: 3645-3653. doi: 10.1098/rstb.2010.0283.

Xiao, L.Q., X.J. Ge, X. Gong, G. Hao, and S.X. Zheng. 2004. ISSR variation in the endemic and endangered plant *Cycas guizhouensis* (Cycadaceae). *Annals of Botany* **94**: 133-138. doi: 10.1093/aob/mch119.

Zhang, X. 2019. Ovule development in Cycads: Observation on anatomy and nucellus morphology in *Zamia* and *Cycas. bioRxiv.* doi: 10.1107/735837.

Zheng, Y., and X. Gong. 2019. Niche differentiation rather than biogeography shapes the diversity and composition of microbiome of *Cycas panzhihuansis. Microbiome* **7.** doi: 10.1186/s40168-019-0770-y.